A Mini Review of Photocatalytic Effects of Nano TiO_2 and an Analysis of Their Effectiveness

MD. Golam Sazid
Nano Research Centre

Asraf Ibna Helal
Nano Research Centre

Islam, Torikul
Nano Research Centre

Purkaystha, Semanto
Nano Research Centre

https://doi.org/10.5109/7157951

出版情報：Proceedings of International Exchange and Innovation Conference on Engineering & Sciences (IEICES). 9, pp.72-78, 2023-10-19. 九州大学大学院総合理工学府
バージョン：

A Mini Review of Photocatalytic Effects of Nano TiO_2 and an Analysis of Their Effectiveness

MD. Golam Sazid[1*], Asraf Ibna Helal[1, 2], Torikul Islam[1], Semanto Purkaystha[1]

[1]Nano Research Centre, Bangladesh
[2]Department of Statistics, Shahjalal University of Science and Technology, Sylhet-3114, Bangladesh
*Corresponding author email: mdgolamsazid@gmail.com

Abstract: *Nanomaterials can improve performance and can be developed in innovative ways, which will impact multiple sectors. Nano TiO_2 is different in behavior from its larger counterparts as the properties rely on size of the materials. TiO_2 nanoparticles (NPs) have a big benefit over other substances because they are small and have a high ratio of surface area to volume. They are great for photocatalysis and can break down a wide range of dyes. As they can act as photocatalysts, TiO_2 NPs are becoming more and more important in environmental uses. Several researchers have used TiO_2 to degrade various dyes. The ability of TiO_2 NPs as photocatalysts depends on several factors, such as their crystalline form, particle size etc. Our systematic review will reveal that the factors that have impact on dye degradation efficiency of TiO_2 where the dyes methylene blue (MB), methyl orange (MO), rhodamine B (RB) are in concern.*

Keywords: NPs; TiO_2 NPs, Photocatalytic activities; Dye degradation.

1. INTRODUCTION

Globally, the dearth of clean and plentiful natural energy, environmental adulteration, and contamination, are among the most pressing issues at present. Rapidly expanding industries have produced effluent carrying heavy metals and several types of organic dyes. These industrial effluents are extremely poisonous and may cause cancer. Additionally, these industrial pollutants contribute to water contamination, which has acute negative effects on aquatic existence and humans [1]. The creation of methods that can transform dangerous, hazardous contaminants into safe chemicals is therefore urgently needed. Nano photocatalysis is regarded as one of the most effective methods for combating the energy crisis and environmental adulteration [2]. A fortunate method for dye elimination involves using nano semiconductor materials revealing high photocatalytic reactivity in the removal of multiple organic compounds without transferring the prime pollutant into a succession of toxic substances. New methods to improve both basic and sophisticated methods of water treatment are provided by nanomaterials [3] [4]. Throughout the course of human history, a wide variety of physical and chemical methods have been effectively utilized and scaled up for the purpose of removing organic contaminants from water sources or degrading them [5]. Nanomaterials have demonstrated remarkable efficacy in the remediation of contaminated water [6]. Titanium dioxide (TiO_2) is such a nanomaterial which was prepared by sol-gel process. Titanium Tetrachloride ($TiCl_4$) has been used for the preparation, and calcination was required at different calcination temperatures [7]. It is possible to remove organic pollutants from water through photolysis using n-type semiconductor metal oxides and TiO_2 [8]. Along with TiO_2 other NPs are also feasible for photocatalytic activity and dye degradation. Zeolitic Imidazolate Frameworks (ZIFs), are a kind of porous metal organic frameworks [9]. These NPs have been employed for the purpose of eliminating heavy metal from water [10]. Hybrid nanostructures consisting of Au and ZnO have the potential to be employed in the field of water treatment for heterogeneous photocatalytic purposes [11]. Recently, nano titanium oxide has been regarded as the best candidate photocatalyst for the degradation and elimination of various harmful organic toxins due to its chemical stability, biocompatibility, high oxidizing power, non-toxicity, and low cost [12] [13] [14]. Crystalline and textural characteristics are regarded as the primary factors that determine the photocatalytic properties of samples. In comparison to other photocatalysts, TiO_2 NPs are regarded as one of the most promising dye treatments photocatalysts due to their nontoxicity, potent oxidizing ability, and high stability. Under UV light, the photocatalytic activity of TiO_2 with a large bandgap of 3.2 eV can generate reactive oxygen species (ROS), such as single superoxide oxygen, anion radical, hydroxyl radical, and per hydroxyl radical (see Fig. 1). These reactive oxygen species catalyze the reaction cascade within the microbial cell, resulting in the destruction of dyes [15]. TiO_2 NPs are efficient in degradation of MB, MO, RB etc. dye. TiO_2 has been performed against MB dye. The particle size was 8.7 nanometer (nm). The degradation efficiency was 97% after 180 minutes [16]. $MnTiO_3$ has been tested against MB dye. The size of the particles was 35.5 nm. After 240 minutes, the reduction in efficiency was 75%. $MnTiO_3/TiO_2$ has been tested against MB dye. The size of the particles was 29.2 nm. After 240 minutes, the decline in efficiency was at 70% [17]. The utilization of Cu-Prophyrin sensitized TiO_2 has been executed in opposition to the MB dye. The magnitude of the particle's dimensions was measured to be 24 nm. Following a duration of 120 minutes, the efficiency of degradation was determined to be 98.70% [18]. In this systematic review, we have taken data from lab-based research papers and utilize these in statistical analysis to find our conclusion. We conduct descriptive analysis and correlation. Here, we find the factor's effect on TiO_2 dye degradation efficiency. For this study we use some statistical analysis such as descriptive analysis, bar-charts, and correlation to fulfill aims of this study. The descriptive analysis and bar-chats will give an overview of dye degradation by TiO_2 NPs. On the other hand, the correlation will show the relationship between efficiency and the variables those have effect on efficiency.

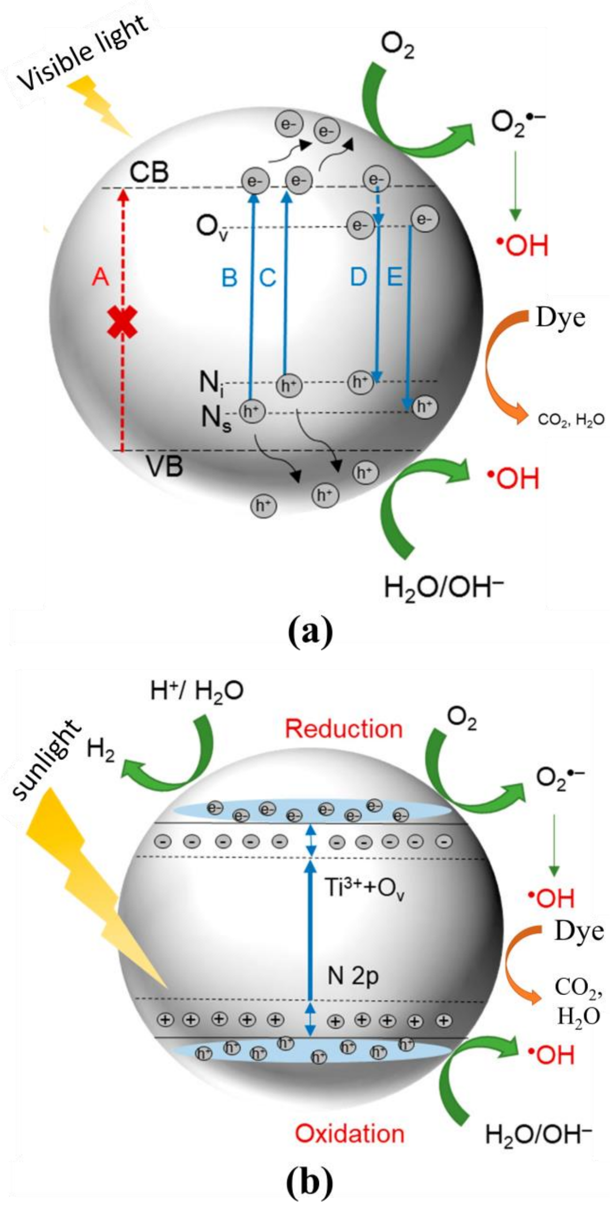

Fig. 1. Photocatalysis by TiO_2 NPs (a) under visible light (b) under sunlight [19]

2. PHOTOCATALYTIC ACTIVITY OF TiO_2 NPS

In the case of degradation, MB dye has been tested with TiO_2/GO. The size of the particles was 12.50 nm. After 45 minutes, degradation efficiency was 98.67% [20]. 0.24%Co/TiO_2 has been tested for MB dye degradation. The size of the particles was measured to be 16.53 nm. After 150 minutes, 80% dye degradation had occurred. [21]. It proves that the size and time are two factors to analyze the efficiency of NPs in the case of dye degradation. There are other works which also show the variation of efficiency and the size and duration of work were the factors for these studies. In a study, the MB dye has been tested using Fe_3O_4@SiO_2/TiO_2/Co/rGO. Particles measured in at 4.9 nm in size. In 160.2 minutes, the efficiency of degradation had reached 98.87% [22]. $ZnFe_2O_4$@SiO_2@TiO_2(ZST)-40 was evaluated against MB dye. The results were positive. The size of the particles was 4.1 nm. The efficiency of the degradation had reached 95.10% after 120 minutes [23]. An experiment involving the use of titanium/silicon at iron catalyst has been conducted in order to assess its effectiveness against MB dye. The size of the particle measured 4 nm. After a duration of 120 minutes, the efficiency of degradation was observed to be 73% [24]. In test of degradation of MB dye, rGO/TiO_2/ZnO was used. It had a size of 13.89 nm. After passing 120 minutes, the degradation efficiency was 92% [25]. 2.0 wt% Ag/TiO_2 was tested against MB dye. The particle size ranged between 30 and 45 nm. After 120 minutes, the decrease in concentration of dye was 82.30% [26]. Another TiO_2 NP has been utilized in opposition to MB dye and the particle size of which was 27.6 nm. After 40.2 minutes, the degradation efficiency was 99 percent. MB dye degradation has also been conducted with $ZnTiO_3$(TZ21). The size of particles was 18.9 nm. After 40.2 minutes, the rate of decomposition was 81.7% [27]. MB dye has been tested with THNF-400 (Titanium Dioxide hollownanofibre). The size of each particle was 234(+/-) 34 nm. After 300 minutes, the rate of degradation was 42.90% [28]. TiO_2 was annealed at 600º C and tested for the degradation of MO dye. There were 15nm-sized particles. After 180 minutes, the degradation efficiency was 87% [29]. After 180 minutes, TiO_2 NPs of the 15 nm had the degradation efficiency as 87% [30]. The efficacy of C_{60}-AuNPs-TiO_2 has been evaluated in relation to its ability to degrade MO dye. The particle was measured as 8 nm sized. After a duration of 160.2 minutes, the efficiency of degradation was found to be 95%. The efficacy of pristine TiO_2 has been evaluated in relation to MO dye. The size of the particle was measured to be 21 nm. The degradation efficiency was determined as 47% following duration of 160.2 minutes [31]. MO dye has been tested using TiO_2/CNF. The size of the particle was 1.0934 nm. The efficiency of the deterioration was 99.72% [32]. MO dye has been tested on a porous polymer with integrated Ag-TiO_2. 16.3 nm was the size of the particles. 180 minutes later, the deterioration efficiency was 81.40%. MO dye has been tested using this particle [33]. Experiments using TiO_2/CF catalyst and MO dye have been conducted. There were 35 nm sized TiO_2/CF particles. After 240 minutes, the degrading efficiency was at 90.02 percent [34]. GO/TiO_2 was tested against MO dye. The size of the particles ranged from 20 to 40 nm. After 240 minutes, the rate of MO dye degradation had reached 85.62 percent [35]. TiO_2 of 11.5 nm size has been evaluated in relation to its ability to degrade MO dye. After a duration of 60 minutes, the degradation efficiency was recorded to be 40.20% [36]. MO dye has been degraded with Ag-CdS@Pr-TiO_2. The size of each particle was 10-30nm. After 30 minutes, 98% of the degradation had been done [37]. TiO_2/ASS was tested for MO dye degradation. The particle size was found, ranged from 15.2 to 29 nm. After 360 minutes, the decline in concentration was 90%. [38]. MO dye has been degraded with TiO_2/ZnO NPs. 4nm was the particulate size. After 30 minutes, the rate of decomposition was 97% [39]. Tests have been done on RB dye degradation with titanium molybdate with size of 43.27 nm. After 150 minutes, 96% of the dye degradation had been done [40]. Experiments using TiO_2@GO for RB dye degradation have been conducted in a study. 10 nm was the particle size. After 120 minutes, the degrading effectiveness was at 100% [41]. The efficacy of TiZnO NPs of 32.3 nm size has been evaluated in degradation of RB dye. The rate of degradation exhibited a remarkable efficiency of 99.29% following a duration of 60 minutes [42]. RB dye degradation has been performed with CNT-TIO_2-450 nano catalyst. The size of the particle was 10.1 nm. The degradation efficiency was 100% after 24.6 minutes [43]. The material was synthesized through the sol-gel method. The efficacy of TiO_2 has been evaluated in relation to its performance against RB dye. The size of the particle was measured to be 2 nm. After a duration of 150 minutes, the efficiency of degradation was found to be 94% [44]. 0.6% Cu-TiO2 was tested against RB dye. The size of the particles was 32.87 nm. After 120 minutes, the degrading efficiency had reached 97% [45]. RB dye has been degraded with a catalyst which is Poly[ANE+N+PMI]-TiO_2 NPs. The size of each particle was 800-1000 nm. After 120 minutes, the decline of concentration of dye was 95% [46]. Degradation of RB with Au-TiO_2 NS was performed in another study. 3 nm was the particle size. After 60 minutes, the degradation efficiency was at 85% [47]. An analysis of RB dye degradation using CNNS/TiO_2 NPs has been carried out. The size of the particles was less than 5 nm. After an hour, the rate of degradation had reached a perfect 100% [48].The performance of N-doped TiO_2 NPs has been evaluated in the degradation of RB dye. The size of the particle was within the range of 80-120 nm. After a duration of 180 minutes, the efficiency of degradation was observed to be 40% [49]. 7-l@TiO_2 has been conducted for degradation of RB dye. The size of the particles was 11.23nm. After 240 minutes, the degradation efficiency was 100 percent [50].

3. METHODOLOGY

We possess a dataset consisting of 54 observations of TiO_2 NPs, intended for statistical analysis. The dataset comprises four distinct variables, namely Size, Efficiency, and Dye name, pertaining to TiO_2 NPs. We conduct a descriptive and correlation in order to enhance the precision of our findings. Additionally, the correlation analysis helps to verify the presence of a statistically significant relationship and identify variables that affect the efficacy of NPs. SPSS-version 25 is utilized for the purpose of conducting data analysis. The variables are rendered categorical for the sake of facilitating data analysis. The categorization of variables is performed for the purpose of facilitating data analysis.

Table 1: Table of categorical variables introduction

Variables Name	Category	Description
Efficiency of NPs	Most Efficient	Which efficiency is greater than 70%
	Efficient	Efficiency 70% or less
Size of NPs	1 is (<30)	Size is 30 nm or less
	2 is (>=30)	Size is above 30
Dye Name	1	MB
	2	MO
	3	RB

4. TABLES OF THE COLLECTED DATA

Table 2: TiO_2 NPs with different dye

Np Name	Size (nm)	Dye	Efficiency	Time (h)	Ref.
TiO_2	8.7	MB	97%	3	[16]
$MnTiO_3$	35.5	MB	75%	4	[17]
$MnTiO_3$/ TiO_2	29.2	MB	70%	4	[17]
Cu-Prophyrin sensitized TiO_2	24	MB	98.70 %	2	[18]
TiO_2/GO	12.50	MB	98.67 %	0.75	[20]
Co/TiO_2	16.53	MB	80%	2.5	[21]
Fe_3O_4@S iO_2/TiO_2-Co/rGO	4.9	MB	98.87 %	2.67	[22]
$ZnFe_2O_4$ @SiO_2@ TiO_2(ZST)-40	4.1	MB	95.10 %	2	[23]
30 Ti/Si@Fe	4	MB	73%	2	[24]
50 Ti/Si@Fe	4	MB	89%	2	[24]
80 Ti/Si@Fe	4	MB	96%	2	[24]
rGO/TiO_2 /ZnO	13.89	MB	92%	2	[25]
Ag/TiO_2	30-45	MB	82.30 %	2	[26]
a-TiO_2(TZ1 0)	27.6	MB	99%	0.67	[27]
$ZnTiO_3$(T Z21)	18.9	MB	81.7 %	0.67	[27]
Disordere d Zn_2TiO_4(TZ11)	6.5	MB	96.10 %	0.67	[27]
Zn_2TiO_4(TZ12)	13.6	MB	82.4 %	0.67	[27]
THNF(Titanium Dioxide hollow nanofiber)-400	236(+/-)34	MB	42.90 %	5	[28]
THNF-500	240(+/-)39	MB	61.70 %	5	[28]

THNF-600	177(+/-)32	MB	85.50 %	5	[28]
600°C annealed TiO_2	15	MO	87%	3	[29]
scoria-Ni/TiO_2	500	MO	95.89 %	0.75	[30]
C_{60}-AuNPs-TiO_2	8	MO	95%	2.67	[31]
Pristine TiO_2	21	MO	47%	2.67	[31]
TiO_2/CNF	1.0934	MO	99.72 %		[32]
Ag-TiO_2 embedded porous polymer (PPTS)	16.3	MO	81.40 %	3	[33]
Ag-TiO_2(TS)	16.3	MO	84.80 %	3	[33]
TiO_2/CF	35	MO	90.02 %	4	[34]
GO/TiO_2	20-40	MO	85.62 %	4	[35]
TiO_2	11.5	MO	40.20 %	1	[36]
CTAg 1	11.7	MO	97.48 %	1	[36]
CTO.2/1	12.4	MO	62.60 %	1	[36]
Ag–CdS@Pr-TiO_2	10-30	MO	98%	0.5	[37]
TiO_2/ASS	15.2-29	MO	90%	6	[38]
TiO_2/ZnO hedgehogs	4	MO	97%	0.5	[39]
Titanium Molybdate	43.27	RB	96%	2.5	[40]
TiO_2@GO	10	RB	100 %	2	[41]
TiZnO	32.3	RB	99.29 %	1	[42]
TiAg	39.4	RB	40.42 %	2	[42]
TiAgZn	61.4	RB	87.73 %	2	[42]
CNT-TiO_2-450	10.1	RB	100 %	0.41	[43]
CNT-TiO_2-350	7.4	RB	91.14 %	0.41	[43]
CNT-TiO_2-550	16.2	RB	79.36 %	0.41	[43]
CNT-TiO_2-650	34	RB	69.41 %	0.41	[43]
CNT-TiO_2-750	36.2	RB	63.58 %	0.41	[43]
CNT-TiO_2-850	38.6	RB	86.02 %	0.41	[43]
sol-gel prepared TiO_2	2	RB	94%	2.5	[44]
Cu-TiO_2	32.87	RB	97%	2	[45]
Poly[ANE+N+PMI]-TiO_2	800-1000	RB	95%	2	[46]
Au-TiO_2 NSPs	3	RB	85%	1	[47]
CNNS/TiO_2	~5	RB	100 %	1	[48]
N-doped TiO_2 NTA	80-120	RB	40%	3	[49]
7-I@TiO_2	11.23	RB	100 %	4	[50]
GR-TiO_2	3-6	RB	98%	1	[51]

5. RESULT AND DISCUSSION

We perform the descriptive analysis and bar-charts in this study to see an overview of related variables in TiO_2 NPs dye degradation.

Table 3: Descriptive Analysis of TiO_2 NPs

Variables	Category	Frequency	Percentages
Size	<30	36	65.5
	>=30	19	34.5
Dye Name	Methylene Blue	20	36.4
	Methyl Orange	15	27.2
	Rhodamine B	20	36.4
Efficiency	Most Efficient	10	18.2
	Efficient	45	81.8

Table 3 shows the descriptive analysis of TiO_2 NPs. Where it is clear that 65.5% of the data belongs to less than 30nm in their sizes, and the rest of the data belongs to above 30. The same percentages of data show their dye degradation activities with Methylene Blue and Rhodamine B dye, which is 36.4%. The percentage of most efficient TiO_2 NPs is 18.2, and the rest, 81.8%, are efficient by their dye degradation.

Figure 2 reveals the percentages of efficient and most efficient TiO_2 NPs are the belonging to their different sized categories. We see that 51.18% of the most efficient NPs' sizes are less than 30 and 23.64% are greater than or equal to 30. On the other hand, 7.27% of efficient TiO_2 NPs' sizes are less than 30, and 10.91% of NPs' sizes are above or equal to 30.

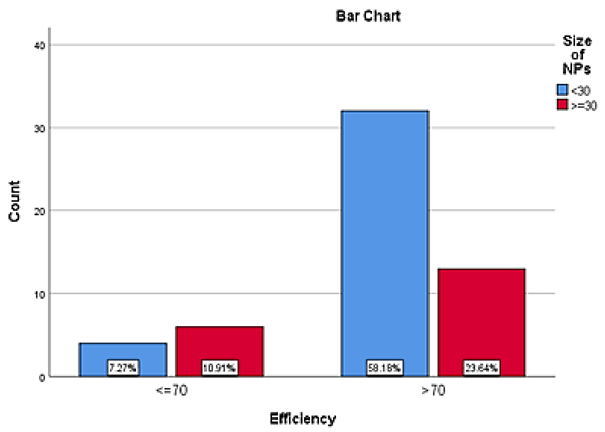

Fig. 2. Size vs Efficiency Bar Chart

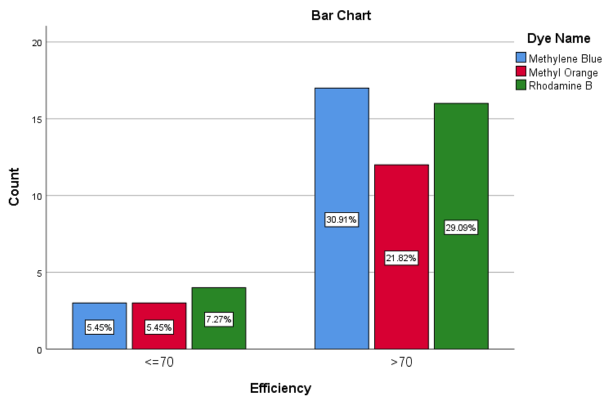

Fig. 3. Dye vs Efficiency Bar Chart

Figure 3 shows that 21.82% of the most efficient TiO_2 NPs in our data degrade methyl orange dye and show their efficiency, whereas 5.45% of the NPs show moderate efficiency by degrading methyl orange dye. The percentage of most efficient NPs and the percentage of efficient NPs in the degradation of Methylene Blue dye are 30.91% and 5.45%, respectively. Also, we see that the percentage of most efficient NPs and rate of efficient NPs in Rhodamine B degradation are 29.09% and 7.27%, respectively.

Now the result of the bivariate correlation helps us to find the relationship between efficiency and those variables which are related to efficiency. That means it reveals variables relation with efficiency of TiO_2 NPs those have impact on the efficiency. The result is as follows:

Table 4: Bivariate Correlation Result

		Sizes of NPs	**Dye Name**	**Efficiency**
Size of NPs	Pearson Correlation	1	.269*	-.252
	Sig. (2-tailed)		.047	.063
	N	55	55	55
Dye Name	Pearson Correlation	.269*	1	-.055
	Sig. (2-tailed)	.047		.689
	N	55	55	55
Efficiency	Pearson Correlation	-.252	-.055	1
	Sig. (2-tailed)	.063	.689	
	N	55	55	55

From Table 4, we see the correlation between efficiency and the other two variables (size and dye name). It reveals that the correlation coefficient between size and efficiency is -0.252. That means there is a moderately negative correlation between size and efficiency. Which means that if the size increases, the efficiency of photocatalysis will decrease. If the size decreases, the efficiency will increase.
And we also see that the correlation between dye and efficiency is -0.55. That means there is a weak relationship between dye and efficiency. Which interprets that for TiO_2 NPs, there is no variation in dye degradation between different dyes.

6. CONCLUSION

Our study of TiO_2 NPs has provided a descriptive analysis. We noticed that the dye was degraded by the NPs in terms of both its size and the time period of degradation. We found that there is a correlation between size and efficiency of dye degradation. The size and efficiency of degradation is in inversely proportional relation. In addition, we found only a shaky connection between the dye and the effectiveness of the TiO_2 NPs at a catalyst. We come to the conclusion that an increase in size will result in a reduction in the photocatalytic activity efficiency. The efficiency will improve in direct proportion to the size reduction of TiO_2 NPs.

7. REFERENCES

[1] G. J. Jiao, J. Ma, Y. Li, D. Jin, J. Zhou, R. Sun, Removed heavy metal ions from wastewater reuse for chemiluminescence: Successive application of lignin-based composite hydrogels, J. Hazard. Mater., 421 (2022) 126722.

[2] S. H. Nipu, N. Neogi, K. P. Choudhury, Advances with Metal Organic Framework based nanomaterials in 4th industrial revolution, Proc. Int. Exch. Innov. Conf. Eng. Sci., 8 (2022) 161–168.

[3] N. Kaneva, A. Bojinova, K. Papazova, Enhanced Removal of Organic Dyes Using Co-Catalytic Ag-Modified ZnO and TiO2 Sol-Gel Photocatalysts, Catalysts, 13 (2023) 245.

[4] R. R. Srivastava, P. K. Vishwakarma, U. Yadav, S. Rai, S. Umrao, R. Giri, P. S. Saxena, A. Srivastava, 2D SnS2 Nanostructure-Derived Photocatalytic Degradation of Organic Pollutants Under Visible Light, Front. Nanotechnol., 3 (2021) 1–13.

[5] A. H. Alneyadi, M. A. Rauf, S. S. Ashraf, Oxidoreductases for the remediation of organic pollutants in water–a critical review, Crit. Rev. Biotechnol., 38 (2018) 971–988.

[6] K. P. Choudhury, T. I. Protik, N. Neogi, S. H. Nipu, CNT based nanomaterials for food industry: a review, Proc. Int. Exch. Innov. Conf. Eng. Sci., 8 (2022) 68–75.

[7] A. J. Haider, R. H. Al-Anbari, G. R. Kadhim, C. T. Salame, Exploring potential Environmental applications of TiO2 Nanoparticles, in: Energy

Procedia., 119 (2017) 332–345.
[8] K. P. Choudhury, N. Neogi, S. H. Nipu, T. I. Protik, A mini overview of miscellaneous uses of TiO_2 based nanomaterials, Proc. Int. Exch. Innov. Conf. Eng. Sci., 8 (2022) 221–227.
[9] C.-W. Tsai, E. H. G. Langner, The effect of synthesis temperature on the particle size of nano-ZIF-8, Microporous Mesoporous Mater., 221 (2016) 8–13.
[10] N. Neogi, K. P. Choudhury, S. H. Nipu, T. I. Protik, Utilization of ZIF based nanomaterials for clean environment purposes, Proc. Int. Exch. Innov. Conf. Eng. Sci., 8 (2022) 323–329.
[11] M. A. Subhan, N. Neogi, K. P. Choudhury, Industrial Manufacturing Applications of Zinc Oxide Nanomaterials: A Comprehensive Study, Nanomanufacturing, 2 (2022) 265–291.
[12] I. Székely, Z. Kovács, M. Rusu, T. Gyulavári, M. Todea, M. Focșan, M. Baia, Z. Pap, Tungsten Oxide Morphology-Dependent Au/TiO2/WO3 Heterostructures with Applications in Heterogenous Photocatalysis and Surface-Enhanced Raman Spectroscopy, Catalysts, 13 (2023) 1015.
[13] X. Jaramillo-Fierro, S. Gaona, J. Ramón, E. Valarezo, Porous Geopolymer/ZnTiO3/TiO2 Composite for Adsorption and Photocatalytic Degradation of Methylene Blue Dye, Polymers (Basel)., 15 (2023) 2697.
[14] L. Ju, D. Hong, X. Jin, H. Liu, X. Yang, L. Nie, Q. Liu, Z. Gao, W. Zhu, Y. Wang, X. Yang, Preparation and Study of Photocatalytic Properties of (M(M=Pt, Ag and Au)-TiO2)@MoS2 Nanocomposites, Inorganics, 11 (2023) 258.
[15] M. Subhan, K. Choudhury, N. Neogi, Advances with Molecular Nanomaterials in Industrial Manufacturing Applications, Nanomanufacturing, 1 (2021) 75–97.
[16] F. Azeez, E. Al-Hetlani, M. Arafa, Y. Abdelmonem, A.A. Nazeer, M.O. Amin, M. Madkour, The effect of surface charge on photocatalytic degradation of methylene blue dye using chargeable titania nanoparticles, Sci. Rep., 8 (2018) 1–9.
[17] S. Alkaykh, A. Mbarek, E. E. Ali-shattle, Heliyon Photocatalytic degradation of methylene blue dye in aqueous solution by MnTiO 3 nanoparticles under sunlight irradiation, Heliyon, 6 (2020) e03663.
[18] Z. M. Abou-Gamra, M. A. Ahmed, Synthesis of mesoporous TiO2–curcumin nanoparticles for photocatalytic degradation of methylene blue dye, J. Photochem. Photobiol. B Biol., 160 (2016) 134–141.
[19] S.T.P.A. Review, M. Janus, K. Szyma, C-,N- and S-Doped TiO_2 Photocatalysts: A Review 1 , (2021).
[20] S. Ahmad, Z. Arshad, S. Shahid, I. Arshad, K. Rizwan, M. Sher, U. Fatima, Synthesis of TiO 2 / Graphene oxide nanocomposites for their enhanced photocatalytic activity against methylene blue dye and ciprofloxacin, Compos. Part B, 175 (2019) 107120.
[21] A. E. Pirbazari, P. Monazzam, B. F. Kisomi, Co/TiO2 nanoparticles: preparation, characterization and its application for photocatalytic degradation of methylene blue, Desalin. WATER Treat., 63 (2017) 283–292.
[22] C. Fu, X. Liu, Y. Wang, L. Li, Z. Zhang, Preparation and characterization of Fe3O4@SiO2@TiO2-Co/rGO magnetic visible light photocatalyst for water treatment, RSC Adv., 9 (2019) 20256–20265.
[23] X. Meng, Y. Zhuang, H. Tang, C. Lu, Hierarchical structured ZnFe 2 O 4 @SiO 2 @TiO 2 composite for enhanced visible-light photocatalytic activity, J. Alloys Compd., 761 (2018) 15–23.
[24] S. G. de Moura, T. C. Ramalho, L.C.A. de Oliveira, L.C.L. Dauzakier, F. Magalhães, Photocatalytic degradation of methylene blue dye by TiO2 supported on magnetic core shell (Si@Fe) surface, J. Iran. Chem. Soc., 19 (2022) 921–935.
[25] N. Raghavan, S. Thangavel, G. Venugopal, Enhanced photocatalytic degradation of methylene blue by reduced graphene-oxide/titanium dioxide/zinc oxide ternary nanocomposites, Mater. Sci. Semicond. Process., 30 (2015) 321–329.
[26] T. Whang, H. Huang, M. Hsieh, J. Chen, Laser-Induced Silver Nanoparticles on Titanium Oxide for Photocatalytic Degradation of Methylene Blue, (2009) 4707–4718.
[27] B. Petrovičová, Z. Dahrouch, C. Triolo, F. Pantò, A. Malara, S. Patanè, M. Allegrini, S. Santangelo, Photocatalytic Degradation of Methylene Blue Dye by Electrospun Binary and Ternary Zinc and Titanium Oxide Nanofibers, Appl. Sci., 11 (2021) 9720.
[28] N. N. Mohammad Jafri, J. Jaafar, N. H. Alias, S. Samitsu, F. Aziz, W. N. Wan Salleh, M. Z. M. Yusop, M. H. D. Othman, M. A. Rahman, A. F. Ismail, T. Matsuura, A. M. Isloor, Synthesis and Characterization of Titanium Dioxide Hollow Nanofiber for Photocatalytic Degradation of Methylene Blue Dye, Membranes (Basel)., 11 (2021) 581.
[29] P. P. Subha, M. K. Jayaraj, Solar photocatalytic degradation of methyl orange dye using TiO 2 nanoparticles synthesised by sol – gel method in neutral medium, J. Exp. Nanosci., 10 (2015) 1106–1115.
[30] M. Pirsaheb, H. Hossaini, S. Nasseri, N. Azizi, B. Shahmoradi, T. Khosravi, Optimization of photocatalytic degradation of methyl orange using immobilized scoria-Ni/TiO2 nanoparticles, J. Nanostructure Chem., 10 (2020) 143–159.
[31] M. T. Islam, H. Jing, T. Yang, E. Zubia, A.G. Goos, R.A. Bernal, C.E. Botez, M. Narayan, C.K. Chan, J.C. Noveron, Fullerene stabilized gold nanoparticles supported on titanium dioxide for enhanced photocatalytic degradation of methyl orange and catalytic reduction of 4-nitrophenol, J. Environ. Chem. Eng., 6 (2018) 3827–3836.
[32] G. Liu, X. Pan, J. Li, C. Li, C. Ji, Facile preparation and characterization of anatase TiO 2 / nanocellulose composite for photocatalytic degradation of methyl orange, J. Saudi Chem. Soc., 25 (2021) 101383.
[33] A. Sabir, T. A. Sherazi, Q. Xu, Porous polymer supported Ag-TiO 2 as green photocatalyst for degradation of methyl orange, Surfaces and Interfaces, 26 (2021) 101318.
[34] C. Wang, Z. Shi, L. Peng, W. He, B. Li, K. Li, Surfaces and Interfaces, 7 (2017) 116–124.
[35] C. Lin, Y. Gao, J. Zhang, D. Xue, H. Fang, J. Tian, C. Zhou, C. Zhang, Y. Li, H. Li, GO/TiO 2 composites as a highly active photocatalyst for the degradation of methyl orange, J. Mater. Res., 35 (2020) 1307–1315.

[36] R. Shan, L. Lu, J. Gu, Y. Zhang, H. Yuan, Y. Chen, B. Luo, Photocatalytic degradation of methyl orange by Ag/TiO2/biochar composite catalysts in aqueous solutions, Mater. Sci. Semicond. Process., 114 (2020) 105088.
[37] A. Singh, A. Ahmed, A. Sharma, C. Sharma, S. Paul, A. Khosla, V. Gupta, S. Arya, Promising photocatalytic degradation of methyl orange dye via sol-gel synthesized Ag–CdS@Pr-TiO2 core/shell nanoparticles, Phys. B Condens. Matter, 616 (2021) 413121.
[38] M. N. Rashed, M. A. Eltaher, A. N. A. Abdou, Adsorption and photocatalysis for methyl orange and Cd removal from wastewater using TiO 2 /sewage sludge-based activated carbon nanocomposites, R. Soc. Open Sci., 4 (2017) 170834.
[39] R. Zha, R. Nadimicherla, X. Guo, Ultraviolet photocatalytic degradation of methyl orange by nanostructured TiO2/ZnO heterojunctions, J. Mater. Chem. A, 3 (2015) 6565–6574.
[40] A. Mobeen, C. M. Magdalane, S. K. J. Shahina, D. Lakshmi, R. Sundaram, G. Ramalingam, A. Raja, J. Madhavan, D. Letsholathebe, M. Maaza, K. Kaviyarasu, C. M. Magdalane, S. K. J. Shahina, D. Lakshmi, R. Sundaram, G. Ramalingam, A. Raja, J. Madhavan, D. Letsholathebe, M. Maaza, et al., Journal Pre-proof, (2019).
[41] M. S. Adly, S. M. El-Dafrawy, S. A. El-Hakam, Application of nanostructured graphene oxide/titanium dioxide composites for photocatalytic degradation of rhodamine B and acid green 25 dyes, J. Mater. Res. Technol., 8 (2019) 5610–5622.
[42] S. Kerli, M. Kavgacı, A. K. Soğuksu, B. Avar, Photocatalytic Degradation of Methylene Blue, Rhodamine-B, and Malachite Green by Ag @ ZnO/TiO2, Brazilian J. Phys., 52 (2022) 22.
[43] Y. Chen, J. Qian, N. Wang, J. Xing, L. Liu, In-situ synthesis of CNT/TiO2 heterojunction nanocomposite and its efficient photocatalytic degradation of Rhodamine B dye, Inorg. Chem. Commun., 119 (2020) 108071.
[44] D. Dodoo-Arhin, F. P. Buabeng, J. M. Mwabora, P. N. Amaniampong, H. Agbe, E. Nyankson, D. O. Obada, N. Y. Asiedu, The effect of titanium dioxide synthesis technique and its photocatalytic degradation of organic dye pollutants, Heliyon, 4 (2018) e00681.
[45] V. Kavitha, P. S. Ramesh, D. Geetha, Synthesis of Cu loaded TiO2 nanoparticles for the improved photocatalytic degradation of Rhodamine B, Int. J. Nanosci., 15 (2016) 1–8.
[46] X. Li, S. Raza, C. Liu, Preparation of titanium dioxide modi fi ed biomass polymer microspheres for photocatalytic degradation of rhodamine-B dye and tetracycline, J. Taiwan Inst. Chem. Eng., 000 (2021) 1–11.
[47] S. A. A. Vandarkuzhali, N. Pugazhenthiran, R. V. Mangalaraja, P. Sathishkumar, B. Viswanathan, S. Anandan, Ultrasmall Plasmonic Nanoparticles Decorated Hierarchical Mesoporous TiO2 as an Efficient Photocatalyst for Photocatalytic Degradation of Textile Dyes, ACS Omega, 3 (2018) 9834–9845.
[48] D. Yang, X. Zhao, Y. Chen, W. Wang, Z. Zhou, Z. Zhao, Z. Jiang, Synthesis of g-C 3 N 4 Nanosheet/TiO 2 Heterojunctions Inspired by Bioadhesion and Biomineralization Mechanism, Ind. Eng. Chem. Res., 58 (2019) 5516–5525.
[49] L. Xia, Y. Yang, Y. Cao, B. Liu, X. Li, X. Chen, H. Song, X. Zhang, B. Gao, J. Fu, Porous N-doped TiO2 nanotubes arrays by reverse oxidation of TiN and their visible-light photocatalytic activity, Surf. Coatings Technol., 365 (2019) 237–241.
[50] R. P. Barkul, M. K. Patil, S. M. Patil, V. B. Shevale, S. D. Delekar, Sunlight-assisted photocatalytic degradation of textile effluent and Rhodamine B by using iodine doped TiO2 nanoparticles, J. Photochem. Photobiol. A Chem., 349 (2017) 138–147.
[51] V. R. Posa, V. Annavaram, J. R. Koduru, P. Bobbala, V. Madhavi, A.R. Somala, Preparation of graphene–TiO2 nanocomposite and photocatalytic degradation of Rhodamine-B under solar light irradiation, J. Exp. Nanosci., 11 (2016) 722–736.